Hindawi
Advances in Materials Science and Engineering
Volume 2022, Article ID 6607683, 14 pages
https://doi.org/10.1155/2022/6607683

Review Article

A Review on Synthesis, Properties, and Environmental Application of Fe-Based Perovskite

G. Jayanthi,[1,2] Sowrirajan Sumathi,[3] Karthik Kannan,[4] V. Andal,[2] and Sivaraj Murugan[5]

[1]Department of Research, Hindustan Institute of Technology and Science, Padur, Chennai 603103, India
[2]Department of Chemistry, KCG College of Technology, Chennai 600100, India
[3]Department of Chemistry, Hindustan Institute of Technology and Science, Padur, Chennai 603103, India
[4]School of Advanced Material Sciences and Engineering, Kumoh National Institute of Technology, Deahak-ro 61, Gumi-si 39177, Gyeongsangbuk-do, Republic of Korea
[5]Department of Mechanical Engineering, Institute of Technology, Hawassa University, Hawassa, Ethiopia

Correspondence should be addressed to V. Andal; andal.che@kcgcollege.com and Sivaraj Murugan; msivaraj2014@gmail.com

Received 19 May 2022; Revised 14 July 2022; Accepted 22 July 2022; Published 20 September 2022

Academic Editor: Gianfranco Carotenuto

Perovskite has attracted the attention of researchers owing to its intriguing physicochemical properties and wide applications. Recently, Fe-based Perovskite as well as its nanoforms is an extensively studied material due to its photocatalytic activity, multiferroic properties, and chemical stability. Fe-based Perovskite exhibits a range of characteristics that become helpful for different applications such as catalysis, electrochemical sensors, and solar cells. This review summarizes the synthesis, properties, and environmental applications of Fe-based Perovskite. This review highlights and provides an overview of the transition metal substituent in Fe-based Perovskite and its properties and how it influences its application in wastewater treatment and catalysis. This article furnishes an overview on synthesis, properties, and environmental application of Fe-based Perovskite.

1. Introduction

Recently, in the materials family, Perovskite materials have attracted the attention of researchers due to their technological significance. Perovskites possess excellent stability and physicochemical, electrical, dielectric, piezoelectric, and superconducting properties which are structure-dependent [1–3]. Hence, they are widely used as catalytic, electric, and magnetic materials [4–6]. Generally, perovskite is represented by the formula ABO_3 and new forms of perovskite include A3B2X9, A2BB/X6, A2BX6, and A4BX6, where A and B are cations and X is a halogen or oxygen anion. The cation and anion compositions of perovskite materials can tune different structures and properties which lead to wide applications [3,7].

The development of nanomaterials and their novel properties enforced the scientists to downsize the perovskite structures to nanoregime to foster its performance and applications [8]. Nanoperovskites have better catalytic efficiency [9] and more enhanced conductivity than bulk due to their large amount of grain boundaries [10], dielectrics [11], and so forth.

Recently, Fe-containing mixed oxides with Perovskite structure, $AFeO_3$($A = Mn$, Co, or Fe), have been studied extensively to develop catalysts to replace precious metals and environmental purification catalysts. Fe-based Perovskites possess good material stability, nonstoichiometric properties, and good phase stability and hence are used as oxygen catalyst [12]. The mixed valence of Fe^{3+} and Fe^{4+} in Perovskite will create ionic mobility and have an effect on catalytic properties [13]. The valence states of Fe in Perovskite are important on the defects and they influence the transport properties such as electrical conductivity [14].

Owing to the interest shown in the Fe-containing Perovskite, this mini-review presents the methods of synthesis, properties, and applications (Scheme 1). This paper

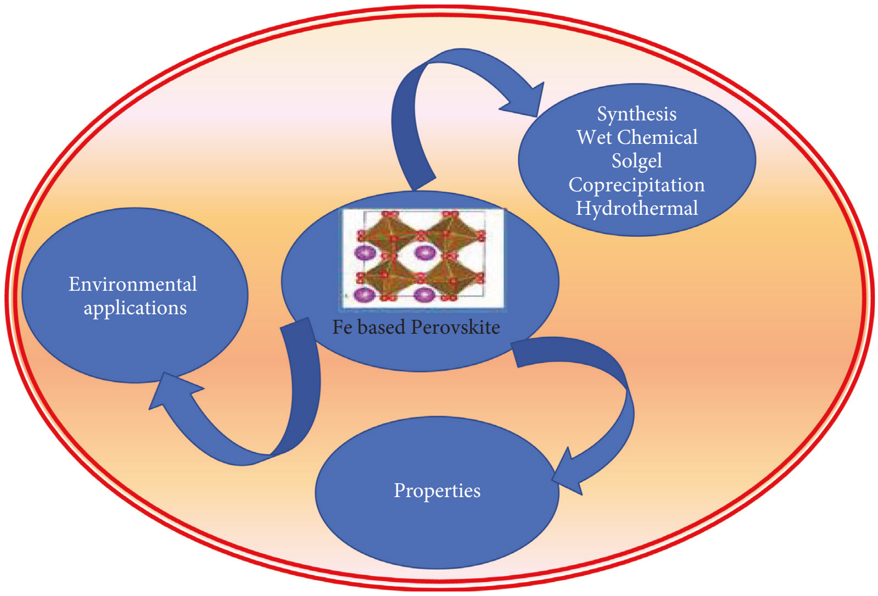

Scheme 1: Schematic representation of the mini-review.

presents an overview on chemical and biological method of synthesis of Fe-based Perovskite. Further, the properties enhancement due to size reduction is detailed. Also, the applications of Fe-containing Perovskite in the field of environment are reviewed.

2. General Synthetic Methods of Fe-Based Perovskites

The synthetic methods of Perovskite play a vital role in designing the structure and properties. Developing an efficient and controllable synthetic method for Fe-based Perovskite is essential to have novel properties with significant applications in environment and so forth. Currently, the research is on the synthesis of Fe-based Perovskite to replace precious metals in the purification process [15].

Various methods of synthesis of Fe-based Perovskite have been reported with different composition and morphologies. Conventional method of synthesis has many disadvantages such as in homogeneity and defects, which makes them unsuitable for various applications. To overcome these disadvantages, new methods have been developed such as wet chemical synthesis, sol-gel, and coprecipitation, hydrothermal, microwave, and biological methods. The synthesis of Fe-based Perovskite is classified into wet chemical and other synthesis routes.

2.1. Wet Chemical Synthesis. Wet chemical synthesis has been extensively used for the synthesis of Fe-based Perovskite nonmaterials of higher surface area at low temperature, including sol-gel, coprecipitation, solvothermal, and hydrothermal. Various researchers made successful attempts and achieved differently structured Perovskite with a large surface area. A few methods generally used for synthesis are overviewed here.

2.2. Sol-Gel Synthesis. The sol-gel method is extensively used for the preparation of Fe-based Perovskite nonmaterial with large surface area. The advantages of this method are inexpensive precursors, simple preparations, and so forth. Among the Fe-based Perovskites, synthesis of $BiFeO_3$ is difficult due to the volatile nature of Bi_2O_3 and it requires a higher temperature. Saira Raiz et al. vanquished it and reported $BiFeO_3$ synthesis using sol-gel method [16]. Theingi et al. have synthesized $LaFeO_3$ nanoparticles by sol-gel method using citric acid with a lower band gap [17]. Liu et al. have synthesized a series of compounds [$CaMnO_3$, $CaFeO_3$, and $CaMn_1$-xFe_xO_3] using the sol-gel method. Citric acid was used as a gelling agent and glycol was added to obtain composition homogeneity and to avoid segregation [18]. Aziz et al. studied the synthesis of GdxMn1−xFe1−yCuyO_3 nonmaterials by sol-gel auto-combustion route [19]. By thermal decomposition of the gel complex of LaFe–(C6H8O7 H_2O), Shabbir et al. reported a unique sol-gel procedure for generating nano-sized Perovskite-type $LaFeO_3$ powder. The scientists discovered that optimizing the gelling conditions leads to the creation of the $LaFeO_3$ Perovskite phase without the need for an explosion or combustion process, as well as pH control. A pure Perovskite phase with a particle size of about 25 nm was found to be above 600°C [20]. Recently, few researchers worked on synthesis of $LaFeO_3$ Perovskite powders by sol-gel method for dye-sensitized solar cell applications. They obtained pure single phase at 850°C by xerogel formation. The flow chart of synthesis is shown in Figure 1.

2.3. Coprecipitation Method. The coprecipitation method is one of the most convenient techniques for synthesizing nano-Perovskite with many components by adding precipitants to get a good degree of homogeneity. Many precipitating agents such as ammonia, NaOH, and amines are used. Among them, ammonia is always preferred because it

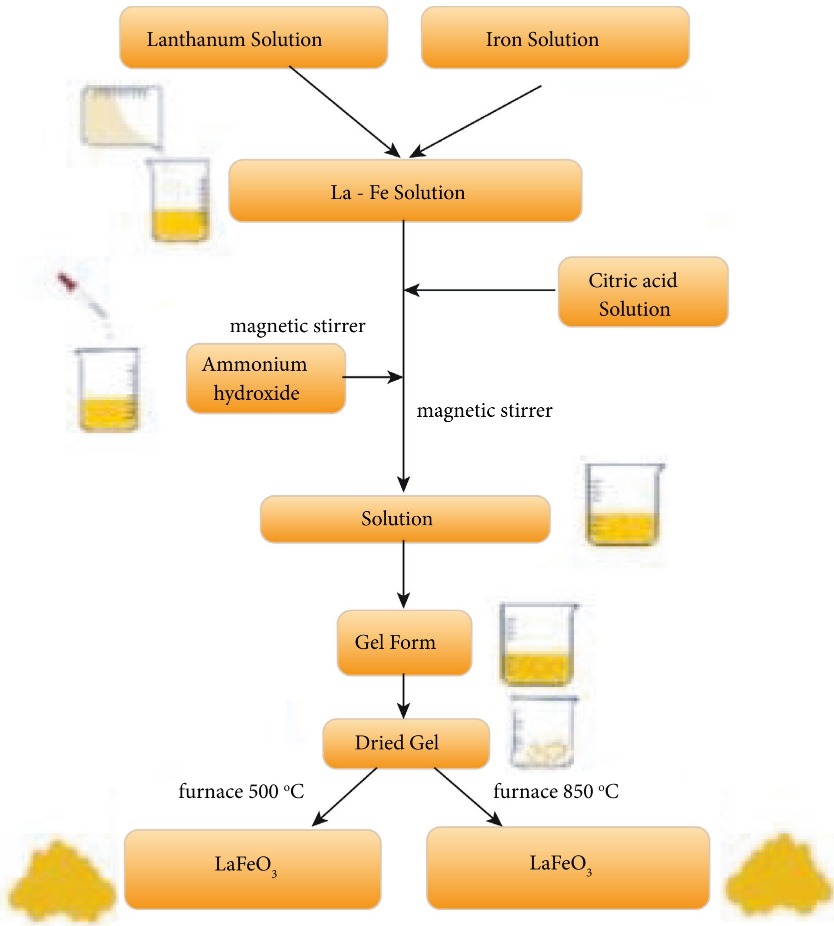

Figure 1: Flow chart of the synthesis of $LaFeO_3$ [21].

can be removed easily upon heating. Temperature, pH, reaction time, speed, and source concentration must all be addressed when using coprecipitation technique. Muneeswaran et al. have synthesized $BiFeO_3$ nanopowder by coprecipitation method using ammonia at pH = 10 [22]. Wang et al. have reported the synthesis of $BiFeO_3$ by coprecipitation method using composite precipitants. The composite precipitants avoid the aggregation of nanoparticles [23]. Khorasani-Motlagh et al. have used octanoic acid surfactant for the synthesis of sphere like $NdFeO_3$ nanocrystals by coprecipitation method [24]. On the basis of A-site and B-site ion selection, several precipitating agents have been reported. Haron et al. synthesized nano-$LaFeO_3$ at 800°C by coprecipitation method using NaOH as precipitating agent. The photograph of the synthesized $LaFeO_3$ is shown in the picture (Figure 2). The synthesis cost was low and no waste was observed in this method [25].

2.4. Hydrothermal Method. The hydrothermal method is a solution reaction-based method. In this method, crystalline structure is obtained for nanomaterials without calcinations. Gómez-Cuaspud et al. synthesized pure phase $LaFeO_3$ Perovskite by the hydrothermal method without calcinations [26]. Single crystal $BiFeO_3$ microplates were developed by hydrothermal method using $C_6H_{10}BiNO_8$ as reductant and surface modifier [27].

Many researchers have recently used the hydrothermal approach to make nano-$BiFeO_3$ Perovskite. The list is as follows: Sazali et al. used biopolymer (chitosan) assisted hydrothermal synthesis of $BiFeO_3$ nanoparticles and got enhanced magnetic properties [28]. Another group used a hydrogen peroxide assisted hydrothermal approach to make shape-controlled $BiFeO_3$ microspheres. To establish an oxygen-rich environment, they employed H_2O_2 [29]. Han et al. also created spindle-like $BiFeO_3$ powders with a width of 0.6 mm and a thickness of 0.3 mm at pH 14 and 200°C for 72 hours, adding a little amount of H_2O_2. Chen and colleagues used an ethanol-assisted hydrothermal technique to make $BiFeO_3$ nanopowders. The ethanol solvent is used extensively in this process to produce pure phase $BiFeO_3$ [30]. On increasing the hydrothermal reaction time from 6 h to 15 h, $BiFeO_3$ microcylinders were obtained by Di et al. [31]. The hydrothermal microwave approach produced $BiFeO_3$ Perovskite crystals with better uniformity than the solid-state reaction method at low temperature of 180°C [32]. Researchers recently used a hydrothermal approach to produce nano-$BiFeO_3$ using different amounts of chitosan biopolymer and KOH as a precipitating agent [28]. Wafer $BiFeO_3$ was synthesized by hydrothermal method without using mineralizer or precipitant.

Figure 2: $LaFeO_3$ powder synthesized by coprecipitation method [25].

Mesbah et al. employed a hydrothermal technique to synthesize nano-$LaFeO_3$ using lanthanum and iron salts in a stoichiometric ratio. To obtain nano-sized $LaFeO_3$, PVP was used as a capping agent, and alkali (NaOH) was added [33].

2.5. Microwave Method. Microwave method is an alternative to the conventional heating method. Microwave heating has higher heating rates and short processing time, which controls the microstructure and better functional properties compared to conventional synthesis [34] of homogeneous Perovskite. Rafael synthesized $Ba_{0.5}Sr_{0.5}Co_{0.8}Fe_{0.2}O_{3-\delta}$ Perovskite by microwave method and achieved same densification as conventional method with less processing time. The grain size obtained was nanoscale compared to conventional method. The microwave hydrothermal synthesis of $BiFeO_3$ crystallites at 467 K for 2 hours was initially reported by Komarneni [35]. Joshi et al. described a simple microwave process for making well-defined single-crystalline Perovskite $BiFeO_3$ nanocubes [36]. Zhu et al. obtained well-dispersed Perovskite BFO nanocrystals under similar experimental circumstances as Joshi's technique, with the exception of a longer reaction period (60 min) [37].

2.6. Crystallography of Fe-Based Perovskite. Perovskite has an ABO_3 form, where B is a transition metal ion with a short radius, bigger A is an alkali earth metal or lanthanide with a larger radius, and O is the oxygen ion in a 1 : 1 : 3 ratio. Atom B is positioned in the cube corner of the ABO_3 Perovskite cubic unit cell, with oxygen atoms positioned in face-cantered positions. Atom A is positioned in the body centre. Size, a shift in oxidation states, and Jahn-Teller processes are three primary concepts that are typically used to explain the distortions in Perovskites. Electroneutrality and the other ionic radii parameters are two prerequisites for Perovskite formation. In accordance with electroneutrality, the Perovskite formula needs to be neutrally balanced, so when the charges of A and B ions are added, the result should be equal to the total charge of the oxygen ions. The radii of A and B ions should be $rA > 0.090$ nm and $rB > 0.051$ nm in accordance with the specifications for ionic radii [38].

Understanding the type of crystallographic defects that regulate the functional characteristics of the Fe-based Perovskite material is crucial for understanding how they affect the material's properties. Marezio and Dernier have explained how the crystal structure of $LaFeO_3$, an Fe-based Perovskite, changes depending on temperature and doping. At room temperature and up to 957°C, the structure of undoped $LaFeO_3$ adopts a Perovskite arrangement that is orthorhombic (space group Pbnm). In the $LaFeO_3$ crystal structure $A = 5.55$ Å, $b = 5.56$ Å, and $c = 7.86$ Å are the edge lengths of the unit cell at room temperature, which contains four structural units ($Z = 4$) [39]. Between 960 and 1005°C, $LaFeO_3$ exhibits a first-order structural phase transition from orthorhombic to rhombohedral. This transition results from the B-site cations' tilting, which changes the magnetic characteristics. Similar to this, a phase change happens when alkaline earth cations dope LaFeO3 at site A. Kotomin and his coworkers have found that though $SrFeO_3$ and $CaFeO_3$ are isoelectronic species, their structural geometry differs due to their distinct ionic radii. Since the ionic radius of Ca^{2+} is lower than that of Sr, it possesses a monoclinic phase. In contrast, $SrFeO_3$ has a cubic structure [40]. Wang et al. observed that, at room temperature, $BiFeO_3$ bulk structure has rhombohedral symmetry with a lattice constant of 5.63 Å. The structure and characteristics of $BiFeO_3$ are changed when sites A and B are substituted. Due to the reduced ionic radii of lanthanide ions relative to Bi3+, when lanthanide ions are substituted to site A of $BiFeO_3$, the phase of the material changes from rhombohedral to orthorhombic. Similar to this, the $BiFeO_3$ structure shifts from rhombohedral to triclinic phase when alkaline earth ions are substituted. Phase change was noticed when site B Fe ions were substituted with ions that had similar ionic radii and electronegativity, such as Ti and Mn [41]. $GdFeO_3$ and $GdFeO_3$ doped with Mn were both produced by the sol-gel method by Maity et al. The orthorhombic phase of $GdFeO_3$ with the Pbnm space group is seen. O type orthorhombic phase, which exhibits decreased unit volume and increased photocatalytic activity, is retained when Fe is replaced with 30 percent Mn [42]. Chandra Sekhar created $MnFeO_3$ using the combustion process. He achieved cubic structure with the space group Ia3, as well as the lattice constant value of $a = 9.40$ which is in good agreement with the JCPDS Card No. 010750894 [43]. Sumalin created $LaFeO_3$ via a polymerized complex technique (Figure 3). The synthesized sample's lattice parameters, $a = 0.5564$ nm, $b = 0.7855$ nm, and $c = 0.5556$ nm, were in good agreement with those of orthorhombic $LaFeO_3$ [44]. In order to create Fe-based Perovskite, a variety of synthetic techniques have been employed, including sol-gel, combustion, and polymerized complex. However, the doping of ions merely modifies the phase, lattice structure, and lattice parameters.

Fe-based Perovskite exhibits a variety of interesting properties like ferromagnetic property as in the case of $BaFeO_3$ and increased ferromagnetism in $(Ba/Ca/Sr)FeO_3$. It showed an enhanced magnetic property with increased magnetic moment which meets the needs of spintronic devices [45]. Although Fe-based Perovskite exhibits a range of properties, the focus of our analysis is on ferromagnetic property, electrical conductivity, and catalytic activity. We chose the aforementioned properties since our analysis is based on environmental applications. In addition, several

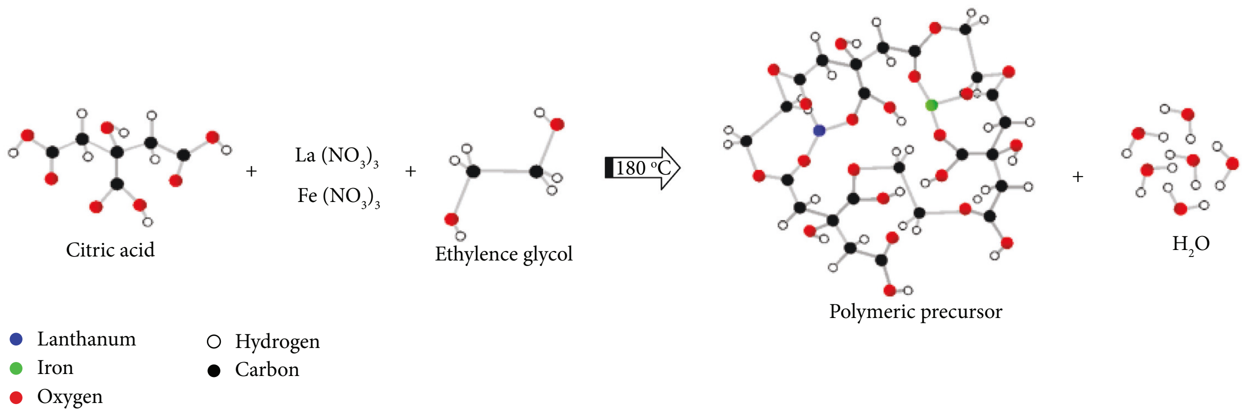

Figure 3: Diagram of the polymeric precursor used in the PC technique to create $LaFeO_3$ nanoparticles [44].

Table 1: Distinctive properties of Fe-based Perovskite.

Distinctive property	Fe-based Perovskite
Ferromagnetic property	$BaFeO_3$, $GdFeO_3$
Electrical conductivity	$SrFeO_3$
Magnetic property	$LaFeO_3$
Catalytic property	$SrFeO_3$, $BiFeO_3$
Ferroelectric	$NdFeO_3$
Electrode	$SmFeO_3$

Fe-based Perovskites exhibit intriguing properties which are shown in Table 1.

2.7. Ferromagnetic Property. Nano-Fe-based Perovskite has superior ferromagnetic properties when compared to bulk materials. Here are a few examples. Due to its heliomagnetic order of wavelength of 62 nm, hollow $BiFeO_3$ nanoparticles display increased ferromagnetic properties when compared to bulk material [46, 47]. Similar to the above reports, wafer-like $BiFeO_3$ also shows ferromagnetic property [48]. Doping with Fe enhances ferromagnetic behavior. Few reports are cited here; Luo and his colleagues looked into the effect of Fe doping on the magnetic properties of Perovskite cobaltite [49].

Fe doping enhances ferromagnetism in the systems of $Pr_{1-y}Ca_yCo_{1-x}Fe_xO_3$ and $Gd_{0.55}Sr_{0.45}Co_{1-x}Fe_xO_3$, while further increasing Fe content suppresses ferromagnetism and results in spin-glass behavior. Alternatively, as long as Fe is doped, ferromagnetism is suppressed in the systems, and no spin-glass behavior is observed in the sample with Fe doping up to 0.3. The phenomenon seen above is thought to be caused by a rivalry between ferromagnetic and antiferromagnetic interactions via intermediate spin. Suresh et al. reported that doping 20% Fe in $SmCrO_3$ decreases the transition of magnetization and flips the magnetization without changing the direction of the applied magnetic field [50]. Manju et al. discovered that replacing Fe/Co in $BaSnO_3$ materials improved the material's ferromagnetic properties. The F centre exchange interactions are responsible for the enhancing attribute [51]. $Bi_{0.5}Na_{0.5}TiO_3$ materials were recently discovered to have ferromagnetism at room temperature. By adding $MgFeO_3$ to the material, ferromagnetism was produced in the source, lowering the band gap from 3.09 eV to 2.43 eV [52]. The magnetic characteristics of Fe doped $BaZrO_3$ were also investigated by Nisar et al. They discovered that doping Fe in the Zr site improves the material's magnetic moment. The material showed enhanced ferromagnetism due to the arrival of unpaired electrons of Fe^{3+} [53]. Rajamani et al. [54] used pulsed-laser deposition to make ferromagnetic $Ba(Ti_{1-x}Fe_x)O_3$ thin films (0.15×0.5) and discovered that the saturation magnetization (MS) increased with the Fe content.

2.8. Electrical Conductivity. In Perovskite-type oxides, electronic conduction is a crucial property. Electronic conduction above R.T. is critical for everyday items, since it assists in the propagation of electrical signals. For solid oxide fuel cells (SOFCs) and solid oxide electrolytic cells, electrode materials with excellent conductivities in both oxidizing and reducing environments are in high demand (SOECs). In the presence of air, many oxide materials have a high conductivity. The key challenge is to find a suitable stable oxide anode material that can conduct well in a reducing environment. To overcome the problem, the researchers are working on Fe-based double Perovskite, and a few literature works are listed below. In a reducing atmosphere, Anikina et al. studied the conductivity of $SrFe_{1-x}Nb_xO_3$, where $x = 0.05$, 0.1, 0.2, 0.3, 0.4, and discovered that $SrFe_{0.9}Nb_{0.1}O_3$ has the highest conductivity. At temperatures below 800°C, however, the conductivity remains below 1 S/cm [55]. Lan et al. studied the conductivity of $SrFe_{0.9}Nb_{0.1}O_3$ and discovered that it has a conductivity of 30 S/cm in a reducing environment, which is significantly greater than previously reported values. In a reducing environment, it was also shown that partially replacing Fe with Cu in $SrFe_{0.9}Nb_{0.1}O_3$ can increase conductivity even further. At 415°C and 5% H_2/Ar, the Perovskite oxide $SrFe_{0.8}Cu_{0.1}Nb_{0.1}O_3$ (SFCN) has conductivities of 63 Scm1 and 60 Scm1, respectively [56].

2.9. Catalytic Property. The high surface activity to oxygen reduction ratio or oxygen activation that resulted from the large number of oxygen vacancies in Fe-based Perovskites was partially responsible for their high catalytic activity. Fe-based Perovskites can be used in a variety of catalytic environmental reactions. The doping of Fe in site B of Perovskites enhances the stability and catalytic activity [57]. Nevertheless, a number of researchers are working on it to expose its features. Using Fe-based Perovskites, photocatalytic water splitting for hydrogen production was researched by many researchers. Vincent and his research team used magnetron sputtering to deposit $LaFeO_3$ film together with g-C_3N_4 in order to study its photocatalytic properties. In comparison to pure $LaFeO_3$, they saw hydrogen generation of 74% at a rate of 10.8 mol/hr/cm^{-2} for $LaFeO_3$/g-C_3N_4 [58]. Similar to this, Iervolina et al. synthesized $LaFeO_3$ catalysts through using solution combustion method with citric acid as the fuel and investigated their photocatalytic properties. For the purpose of generating hydrogen, they investigated into the photocatalytic degradation of glucose solution. They found that increasing the amount of citric acid by twofold boosts the $LaFeO_3$ surface area and the photocatalytic property of hydrogen generation [59]. Ibrahim successfully created n-type $LaFeO_3$ Perovskite using the sol-gel process. He looked into the hydrogen-generating photocatalytic property and developed a low-cost, robust photoelectrochemical cell for solar energy conversion [60].

The photocatalytic degradation of dyes using Fe-based Perovskite is also being researched due to its high stability, nontoxicity, and small band-gap energy. Ismail synthesized $LaFeO_3$ using the sol-gel method and investigated its photocatalytic ability to degrade 4-chlorophenol (4-CP) and rhodamine B (RhB). He noticed that $LaFeO_3$ that has been calcined at 700°C has the highest photocatalytic activity [61]. For the photocatalytic degradation of rhodamine B (RhB) and p-chlorophenol under visible light irradiation, Pirzada et al. developed $LaFeO_3/Ag_2CO_3$ nanocomposites by coprecipitation technique. Under natural sunlight, they achieved degradation efficiencies of 99.5 percent for RhB and 59 percent for p-chlorophenol in less than 45 minutes [62]. To increase the photocatalytic activity of $LaFeO_3$, Vijayaraghavan developed a composite made of $LaFeO_3$ nano-Perovskite-RGO-NiO. By conducting a research study on Congo red dye degradation and hydrogen and oxygen evolution by water splitting, the photocatalytic property of the composite was investigated [63]. The mechanism of the photocatalytic dye degradation and water splitting by $LaFeO_3$ is depicted in Figure 4.

Microwave-prepared $BiFeO_3$ and $LaFeO_3$ were examined for their photoelectrochemical properties. $LaFeO_3$ showed stronger water splitting than $BiFeO_3$ because of the Jahn-Teller distortion, which leads to charge separation [64]. Kim and his coworkers investigated the Fe doping in Co-based Perovskite oxide and explored its catalytic activity towards oxygen evolution reaction in alkaline media. They found that incorporation of Fe in site B doping enhances OER efficiency and stability and showed intrinsic properties too [65]. Because of their intrinsic activity, distinct physicochemical features, and diverse compositions, Fe-based Perovskite oxides have attracted a lot of attention as a potential kind of noble-metal-free candidates for hydrogen evolution reaction (HER) at the cathode [66].

2.10. Environmental Applications. Fe-based Perovskites possess excellent thermal stability and catalytic properties, which make them a potential candidate for environmental applications. In synthetic methods, the substitution of cations in sites A/B is the aspect that induces the catalytic properties in Fe-based Perovskite [67]. Fe-based Perovskites are of low cost and they possess excellent activity in the remediation of pollutants from the environment. Fe-based Perovskites are used for sensing the environmental pollutants in gaseous form. Few examples are cited below.

2.10.1. Fe-Based Perovskite as Sensor. Detecting and monitoring the toxic gases are important for environment protection. Gas sensors are of low cost and they are better alternative to the existing analytical techniques. The increasing demand of highly selective and sensitive sensors has urged the researchers to focus on Fe-based Perovskite as sensor due to its thermal and chemical stability. Fe-based Perovskites have been used for sensing various gases such as carbon monoxide (CO) and oxygen (O_2), and various Fe-based Perovskite and transition metal substituted Perovskite have been used as a sensor for detecting gases which are shown in Table 2. Lanto et al. have studied the gas sensing property for $LaFeO_3$, Sr, and Mg modified $LaFeO_3$ nanoparticles. They found that modified $LaFeO_3$ showed less sensitivity to CO, C_2H_4, and CH_4 compared to unmodified $LaFeO_3$ [68]. Recently, Fabio developed a gas sensor for detecting CO gas using Ti substituted lanthanum ferrite Perovskite ($LaFe_{0.8}Ti_{0.2}O_3$) [69]. Since it has a low band-gap energy, it does not show any ionic domain and is capable of detecting gases under any reducing/oxidizing pressure range. $Bi_5Ti_3FeO_{15}$ nanoparticles were synthesized and their gas sensing properties were studied. Jamil found that it was selective towards oxygen when tested in the presence of other gases and alcohols and proposed as a practical oxygen sensor. The gas sensing setup is depicted in Figure 5 [70]. 2% weight Pd doped $LaFeO_3$ prepared by Xiao Feng et al. showed good response for detecting low concentration of acetone [71]. Wang et al. prepared $LaFeO_3$ nanocrystalline powders by sol-gel method for sensing carbon dioxide gas [72]. Cao and coworkers reported the ethanol gas sensing property of chlorine doped $LaFeO_3$ nanocrystals [73]. Ma et al. prepared mesoporous hollow $PrFeO_3$ (praseodymium ferrite) nanofibers by electrospinning method and studied its sensing property towards acetone [74]. Chen et al. used lotus leaf as biotemplate for synthesizing Ag-$LaFeO_3$ nanoparticles. They also found that the synthesized nanoparticle (Ag-$LaFeO_3$) exhibits enhanced xylene gas sensing property [75]. Similarly, Han et al. also prepared $SmFeO_3$ nanofibers using electrospinning method for the detection of ethylene glycol [76]. Perovskite Ag-$LaFeO_3$ nanofibers were prepared by Wei and coworkers for sensing HCHO gas which is a toxic VOC [77]. Based on the above research, Yang et al. also developed porous $LaFeO_3$ for HCHO sensing at125°C [78].

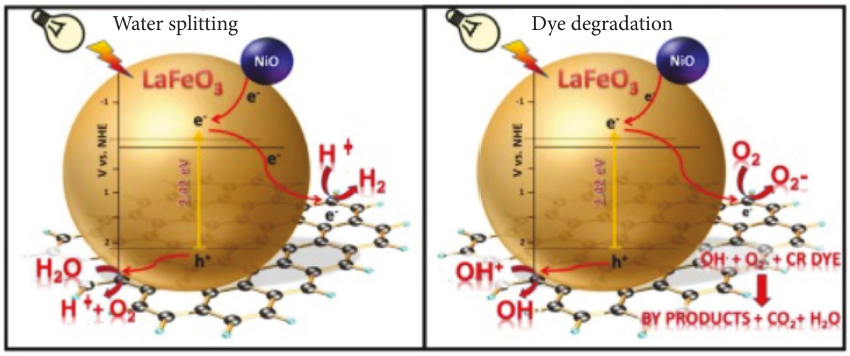

FIGURE 4: $LaFeO_3$'s mechanism for water splitting and dye degradation [63].

TABLE 2: The use of Fe-based Perovskites as sensors for detecting various environmental pollutants.

Fe-based Perovskite	Detecting pollutant	Pollutant limit (ppm)	Form of Perovskite	Reference
$EuFe_{0.9}Co_{0.1}O_3$	Acetone		Powder	[80]
$LaFeO_3$	CO2	2000	Powder	[72]
Chlorine doped $LaFeO_3$	Ethanol		Powder	[73]
$PrFeO_3$ nanofibers	Acetone	500	Nanofibers	[74]
Ag-$LaFeO_3$	Xylene	10	Powder	[75]
$SmFeO_3$	Ethylene glycol	5	Nanofibers	[76]
Ag-$LaFeO_3$	HCHO		Nanofibers	[77]
$LaFeO_3$	HCHO		Powder	[78]
$LaFeO_3$	Sulphur		Powder	[79]
Ca doped $BiFeO_3$	Hydrogen	500	Thin film	[81]
$BiFeO_3$	Carbon monoxide	30	Powder	[82]
$BiFeO_3$	Sulphur	Low	Powder	[83]
$SmFeO_3$	Acetylene	2–80	Thin film	[84]
$LaFeO_3$	NOx	5	Thin film	[85]

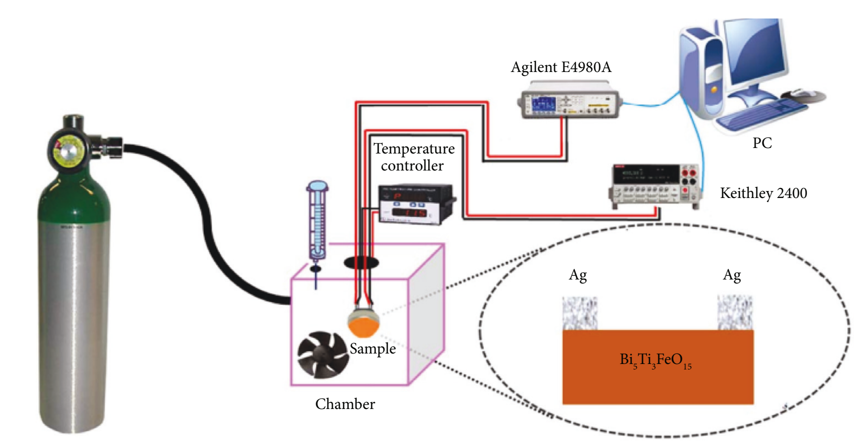

FIGURE 5: Gas sensing setup of $Bi_5Ti_3FeO_{15}$ [70].

Similarly, Queral to et al. [79] synthesized the $LaFeO_3$ nanofibers by calcination at 600°C for the sensing of sulphur containing gases.

2.10.2. Fe-Based Perovskite as Adsorbent. Adsorption is one of the effective, economical, and cheap methods of removing pollutant from wastewater. Adsorption depends on various factors such as surface area, porosity, size distribution, density, and surface charge. Growing demand on adsorbents has led the researchers to focus on nanoparticles due to its high surface-to-volume ratio [86, 87]. Researchers are doing effective research to develop adsorbents of low cost with high adsorption capacity [88, 89]. In view of this, Fe-based Perovskite nanoparticles are considered to be an effective adsorbent because they possess excellent structure and they are employed for the adsorption of pesticides, dyes, heavy metal ions, and volatile organic compounds (Table 3).

The adsorption of various dyes by Fe-based Perovskite was also investigated. Shima capped $La_{0.9}Sr_{0.1}FeO_3$ nano-

Table 3: The use of Fe-based Perovskite as adsorbent for dyes and heavy metal ions.

Fe-based Perovskite	Adsorbing pollutant	Contact time	Removal	Reference
CTAB-capped $La_{0.9}Sr_{0.1}FeO_3$	Anionic Congo red	—	97%	[90]
$SrFeO_{3-\delta}$	Bisphenol A and acid orange 8	24 hrs	83%	[91]
$NdFeO_3$	As(V)	—	126.58%	[92]
$CuFe_2O_4$/PMS	As(III)	—	63.9 mg g^{-1}	[93]
$LaFeO_3$-ACF	Rhodamine B	—	182.6 mg g^{-1}	[94]
$Gd_{0.5}Sr_{0.5}FeO_3$	Methylene blue	—	—	[95]

Perovskite with CTAB and was applied as an adsorbent for the removal of Congo red dyes in aqueous and real samples [90]. He also optimized the adsorption process with various factors such as pH, contact time, dye concentration, and temperature. He proposed that $La_{0.9}Sr_{0.1}FeO_3$ showed 10 times higher adsorption capacity than the pure one. Ming explored strontium ferrite nano-Perovskite for the degradation of organic pollutants Bisphenol A and acid orange without any stimulants under dark condition. He achieved efficient results and further stressed that strontium ferrite nano-Perovskite can be an alternative material for low-cost water treatment [91]. Recently the adsorption of rhodamine B by $LaFeO_3$-ACF was reported by Deng et al. [94]. They prepared activated carbon fibers (ACF) from cotton waste and decorated on $LaFeO_3$ by sol-gel and thermal treatment. The adsorption efficiency of $LaFeO_3$-ACF was higher compared to $LaFeO_3$ due to the electrostatic interaction, hydrogen bonding, π-π stacking, and cation-π interactions. The adsorption of methylene blue dye from water by $Gd_{0.5}Sr_{0.5}FeO_3$ Perovskite synthesized from sol-gel method was reported [95]. The adsorption of heavy metals by Fe-based Perovskite was also explored. The adsorption of As(V) by $NdFeO_3$ synthesized by the polymeric gel precursor method was reported [92]. Removal of As(III) from the water was faster and more efficient by $CuFe_2O_4$/PMS Perovskite than by $CuFe_2O_4$ [93].

Recently, in the field of photocatalysis, Perovskite-based catalysts have grabbed great attention from researchers. Fe-based Perovskite exhibits an excellent visible light-driven photocatalytic property. $LaFeO_3$ showed an excellent and better photocatalytic property than Fe_2O_3 [96]. Doping of Mn in $LaFeO_3$ and its photocatalytic property is investigated. The doping enhances the photocatalytic property [97]. $BiFeO_3$ was also used as a photocatalyst due to the electron-hole separation. Doping of metals in $BiFeO_3$ and its influence on photocatalytic property was also investigated. Gd and Ca doped $BiFeO_3$ showed enhanced photocatalytic degradation of dyes [98, 99]. Further studies have to be explored on the enhancement of photocatalytic studies of $BiFeO_3$. Similarly, Jaffari et al. also prepared the Pd doped $BiFeO_3$ microcomposite by hydrothermal technique. The prepared composite has coral-shaped $BiFeO_3$ surface loaded with spherical Pd nanoparticles, which exhibits more enhanced photoactivity than pure $BiFeO_3$. The enhanced photoactivity is due to the Pd dopant, and the composite possesses excellent recyclability with minimum leakage of Pd after six runs. They also proposed that Pd doped $BiFeO_3$ microcomposite exhibits as potent antimicrobial agent [100].

Sydorchuk et al. recently have investigated the photocatalytic properties of $PrCo_{1-x}Fe_xO_3$ Perovskite powders [101]. Their studies were focused on the influence of structure and its composition on photocatalytic properties.

Researchers also reported that $GaFeO_3$ has good water splitting capacity without any cocatalyst [102]. Another report states that $YFeO_3$ has four times enhanced photocatalytic activity than TiO_2:P25 [103]. Fe-based Perovskite is extensively applied as an environmental catalyst due to its magnetic recovery. Thirumalai Rajan and his coworkers prepared floral-like $LaFeO_3$ nanostructures by surfactant assisted hydrothermal method. The prepared floral $LaFeO_3$ nanostructure was used for degradation of rhodamine B (RhB) and methylene blue (MB) under visible light irradiation [96].

2.10.3. Fe-Based Perovskite as Catalyst. Advanced oxidation processes (AOPs) have emerged in recent years as efficient and effective wastewater treatment technologies. Photocatalysis has risen to prominence among the AOPs as a promising technology for addressing environmental issues. Perovskite and Perovskite-related materials are third-generation photocatalysts which fit into the photocatalytic characteristics by establishing a stable structure and solid solution with a variety of metal ions to achieve the required band engineering for photoelectrocatalytic applications [67]. Fe-based Perovskite serves as a visible light photocatalytic material owing to its low cost and small band-gap compared to the titanium-based Perovskite [104]. In the field of environmental remediation, ferrite-based Perovskites have proven to be promising materials for photocatalytic and photoelectrocatalytic applications. The magnetic and electrical properties of ferrite-based Perovskite draw interest. Due to a distortion in their crystal structures, they feature an intrinsic electric dipole moment, which enhances the separation of photo-generated charges during the photoexcitation process [105].

The production of electrons and holes on the surface of the catalyst causes photocatalytic degradation of dyes. The adsorbed compounds will undergo redox reaction with the produced electrons and holes on the catalyst [106]. The properties of the nanostructured Perovskite material are influenced not only by the composition but also by the structure, morphology, phase, shape, and size. Keeping in its view, Thirumulairajan et al. used a hydrothermal process to make $LaFeO_3$ in three different shapes: nanocubes, nanorods, and nanospheres. The efficacy of the produced nanostructures on photocatalytic degradation of rhodamine dye is being investigated. They found that $LaFeO_3$ nanostructures have better photocatalytic activity. Nanospheres, on the other

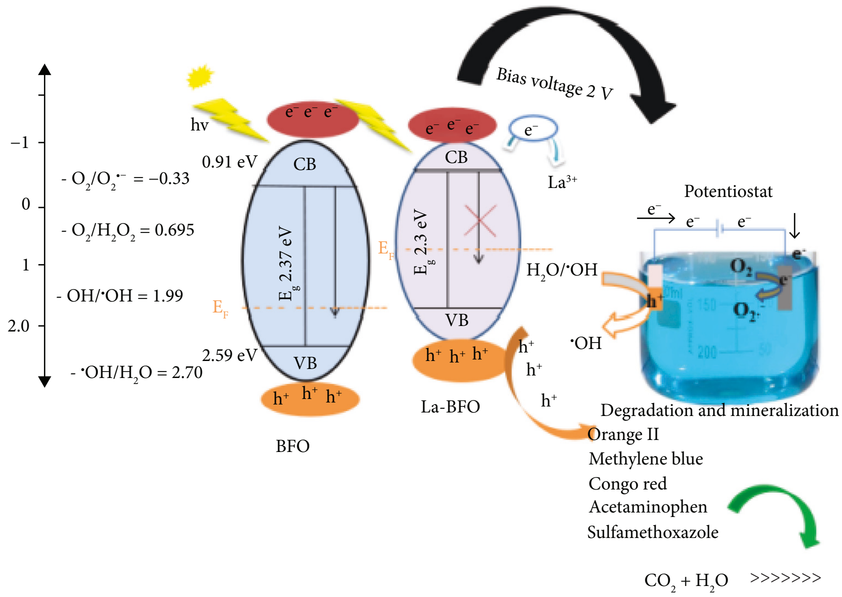

Figure 6: Schematic representation of photoelectrocatalytic degradation of dyes and pharmaceutical pollutants using $BiFeO_3$ and 10% La doped $BiFeO_3$ [113].

hand, were shown to be more efficient than TiO_2 [96]. Similarly, the same researchers prepared floral nanostructured $LaFeO_3$ with a band-gap of 2.10 eV, which showed better photocatalytic efficacy in decomposing rhodamine B and methylene blue when compared to bulk $LaFeO_3$ [107].

Doping of Fe-based Perovskite at both sites gives higher photocatalytic efficiency by reducing the band-gap. The smaller the band-gap, the more visible light absorption for photocatalytic degradation due to e-hole recombination. For example, Hu et al. investigated the photocatalytic property of Sm doped BFO nanoparticles for the degradation of MO under visible light, finding a reduced energy band-gap of 2.06 eV [108]. In the presence of H_2O_2, the visible light photodegradation of MB dye by BFO doped with Ba, Na, and K metal ions was also studied [109]. Jaffari et al. examined the photocatalytic degradation of malachite green dye and phenol from wastewater by doping Pb in BFO nanomaterial. In comparison to bulk BFO and TiO_2, they discovered that Pb substitution increased photocatalytic efficiency. The increased photoactivity was attributed to the suitable Pb concentration, which increased the trapping capability, which aided in the formation and transmission of the produced e-h+ pairs [110]. Similarly, Dy doping in BFO material resulted in MB degradation of 92 percent [111]. The photocatalytic efficiency of Perovskite is improved by Fe doping. The photocatalytic degradation of RNL azo dye was investigated using Fe doped $BaSnO_3$. Fe doping in $BaSnO_3$ creates intermediate levels in the band-gap, trapping electrons and preventing electron-hole recombination, and increasing photocatalytic efficiency [112].

Compared to photocatalytic degradation of organic pollutants, photoelectrochemical degradation is found to be more advantageous. Fe-based Perovskites are playing a key role in degrading the organic pollutant as photoelectrocatalyst. Reports on Fe-based Perovskite as photoelectrocatalyst are meager. Nkwachukwu et al. synthesized La doped $BiFeO_3$ by hydrothermal method and studied its photoelectrocatalytic degradation property on dyes (Orange II, Congo red, and methylene blue) and pharmaceutical pollutants (acetaminophen and sulfamethoxazole). 10% La doping has enhanced the photoelectrocatalytic efficiency by reducing the band-gap. The schematic representation of its mechanism and photoelectrocatalytic efficiency is given in Figure 6 [113].

The principal pollutant responsible for ozone depletion in the stratosphere is nitrous oxide. Infrared radiation is also absorbed by N_2O, which contributes to the greenhouse effect. Thus, one of the key research areas in environmental catalysis is to control N_2O emissions from industries [114]. Although there are a few strategies for reducing N_2O emissions, direct catalytic decomposition is thought to be a simple method for removing the gas. Because of their low cost and high thermal stability, Fe-based Perovskites are applied as a suitable catalyst for N_2O reduction and decomposition reactions.

By doping $BaTiO_3$ with Fe, the photoelectrochemical activity is increased. BaTiO3 showed improved photoelectrochemical activity for hydrogen generation after being doped with Fe [115]. Several research groups have produced numerous $BiFeO_3$ nanostructures and investigated their photoelectrochemical characteristics. Photo-induced water oxidation activity of single-crystalline $BiFeO_3$ nanocubes was discovered by Joshi et al., implying that BFO could be a promising material for photocatalytic applications [36]. For photoelectrochemical water splitting, $BiFeO_3$ was produced and employed as a photocatalyst [116].

Fe-based Perovskites have been extensively investigated as oxidation catalysts due to their oxygen-carrying capacity. Larger $LaFeO_3$ crystals have a smaller band-gap and consequently a weak O–Fe bond strength, leading to increased methane conversion activity and a large amount of detachable O [117]. Researchers have discovered $LaFeO_3$ and $La_{0.8}Sr_{0.2}FeO_3$ Perovskites with low oxygen mobility as promising partial oxidation selective catalysts, but $La_{0.5}Sr_{0.5}Fe_{1-x}Co_xO_3$ ($x = 0, 0.5, 1$) Perovskites with high oxygen mobility are well suited to methane total combustion [118].

The optical properties of Perovskite are enhanced by dopants. The capacity of Fe doping in Perovskites to improve the oxygen evolution reaction is explored here. The significance of Fe in improving OER activity and stability has remained a mystery until now.

After replacing Fe^{3+} in the $LaFeO_3$ Perovskite with Cu^{2+} and Ni^{2+}, the catalytic activity for the N_2O decomposition reaction enhanced. The catalytic activity was further boosted by increasing the reaction temperature. In the case of Ni- and Cu-included $LaFeO_3$ samples, the increased oxygen mobility and minor increase in surface area resulted in the establishment of additional active sites for N_2O adsorption and then decomposition [119]. Fe-based Perovskites as photocatalysts are commonly associated with separation, regeneration, and recycling challenges, despite their favourable and prospective green environmental photocatalytic uses.

3. Conclusion and Outlook

It has been proven in recent years that Perovskites offer the ideal combination of properties to use for environmental issues. Fe-based Perovskites have been synthesized and applied for environmental remediation. For use in environmental applications, more works must still be put into developing Fe-based Perovskites with superior efficiency and great stability. To satisfy the demands of large-scale synthesis for industrial manufacturing, a Perovskite synthetic process that is easier to use and more productive is still required.

The ability of Fe-based Perovskites to remove new pollutants through photocatalysis is currently of significant interest. A wide variety of synthetic techniques are required to create novel materials that improve photocatalytic activity.

Reports on adsorption and degradation of pollutants showed the efficiency of Fe-based Perovskite. Although many compounds are reported on photocatalytic property, there is no detailed study report. The influence of structure, doping, and composition on the photocatalytic property has to be explored further. Fe-based Perovskite exhibits ferroelectric and ferromagnetic properties, and how it influences photocatalytic property is not investigated. Further understanding is needed for an efficient Fe-based Perovskite photocatalyst. There are few reports on the Fe-based Perovskite as sensor, adsorbent, and photocatalyst. Further effort is needed for the synthesis of Fe-based Perovskite as an upcoming future material for environmental applications.

The cost-effectiveness of the design of Fe-based Perovskite-based devices is still a concern for the researchers. For the design and development of nano-Perovskite sensors, catalysts, and adsorbents for environmental implications, several scientists are currently working on Fe-based Perovskites.

Data Availability

All data used to support the findings of this study are included within the article.

Conflicts of Interest

The authors declare that they have no conflicts of interest.

Acknowledgments

The authors would like to express heartfelt thanks to KCG College of Technology for providing support during this research.

References

[1] Y. Wei, Z. Cheng, and J. Lin, "An overview on enhancing the stability of lead halide perovskite quantum dots and their applications in phosphor-converted LEDs," *Chemical Society Reviews*, vol. 48, no. 1, pp. 310–350, 2019.

[2] W. J. Yin, B. Weng, J. Ge, Q. Sun, Z. Li, and Y. Yan, "Oxide perovskites, double perovskites and derivatives for electrocatalysis, photocatalysis, and photovoltaics," *Energy & Environmental Science*, vol. 12, no. 2, pp. 442–462, 2019.

[3] L. Wang, H. Zhou, J. Hu et al., "A Eu 3+ -Eu 2+ ion redox shuttle imparts operational durability to Pb-I perovskite solar cells," *Science*, vol. 363, no. 6424, pp. 265–270, 2019.

[4] Z. Shi, J. Guo, Y. Chen et al., "Lead-free organic–inorganic Hybrid perovskites for photovoltaic applications: recent Advances and Perspectives," *Advanced Materials*, vol. 29, p. 1605005, 2017.

[5] F. Li, M. J. Cabral, B. Xu et al., "Giant piezoelectricity ofSm-doped Pb(Mg1/3Nb2/3)O3-PbTiO3 single crystals," *Journal of Chemical Information and Modeling*, vol. 53, no. 9, pp. 1689–1699, 2019.

[6] B. Arun, V. R. Akshay, and M. Vasundhara, "Observation of enhanced magnetic entropy change near room temperature in Sr-site deficient La0.67Sr0.33MnO3 manganite," *RSC Advances*, vol. 9, no. 41, pp. 23598–23606, 2019.

[7] R. Saha, A. Sundaresan, and C. N. R. Rao, "Novel features of multiferroic and magnetoelectric ferrites and chromites exhibiting magnetically driven ferroelectricity," *Materials Horizons*, vol. 1, no. 1, pp. 20–31, 2014.

[8] N. Phung and A. Abate, "The impact of nano- and micro-structure on the stability of perovskite solar cells," *Small*, vol. 14, no. 46, p. 1802573, 2018.

[9] N. Rezlescu, E. Rezlescu, C. Doroftei, P. D. Popa, and M. Ignat, "Nanostructured lanthanum manganite perovskites in catalyst applications," *Dig. J. Nanomater. Biostructures*, vol. 8, no. 2, pp. 581–587, 2013.

[10] A. M. Ferrari, T. O. Germiniano, J. E. Savoia, R. G. Marques, V. AdS. Ribeiro, and A. C. Ueda, "CaTiO3 perovskite in the photocatalysis of textile wastewater," *Ambiente & Água - An Interdisciplinary Journal of Applied Science*, vol. 14, p. 1, 2019.

[11] W. F. Zhang, J. Tang, and J. Ye, "Photoluminescence and photocatalytic properties of SrSnO3 perovskite," *Chemical Physics Letters*, vol. 418, no. 1–3, pp. 174–178, 2006.

[12] D. N. Mueller, R. A. De Souza, H. I. Yoo, and M. Martin, "Phase stability and oxygen nonstoichiometry of highly oxygen-deficient perovskite-type oxides: a case study of (Ba, Sr)(Co, Fe)O 3-δ," *Chemistry of Materials*, vol. 24, no. 2, pp. 269–274, 2012.

[13] N. A. Merino, B. P. Barbero, P. Ruiz, and L. E. Cadús, "Synthesis, characterisation, catalytic activity and structural stability of LaCo1-yFeyO3±λ perovskite catalysts for combustion of ethanol and propane," *Journal of Catalysis*, vol. 240, no. 2, pp. 245–257, 2006.

[14] C. McCammon, "Crystal chemistry of iron-containing perovskites," *Phase Transitions*, vol. 58, no. 1-3992, pp. 1–26, 1996.

[15] Y. Li, Q. Li, H. Wang, L. Zhang, D. P. Wilkinson, and J. Zhang, "Recent progresses in oxygen reduction reaction electrocatalysts for electrochemical energy applications," *Electrochemical Energy Reviews*, vol. 2, no. 4, pp. 518–538, 2019.

[16] F. Majid, S. T. Mirza, S. Riaz, and S. Naseem, "Sol-gel synthesis of BiFeO3 nanoparticles," *Materials Today Proceedings*, vol. 2, no. 10, pp. 5293–5297, 2015.

[17] M. Theingi, K. T. Tun, and N. N. Aung, "Preparation, characterization and optical property of $LaFeO_3$ nanoparticles via sol-gel combustion method," *SciMedicine Journal*, vol. 1, no. 3, pp. 151–157, 2019.

[18] C. Liu, W. Wang, and D. Chen, "Hydrogen-rich syngas production from chemical looping gasification of biomass char with CaMn1- $xFexO_3$," *Energy & Fuels*, vol. 32, no. 9, pp. 9541–9550, 2018.

[19] A. Aziz, E. Ahmedb, M. NaeemAshiqc et al., "Impact of Gd and Cu substitution on dielectric and magnetic properties of $MnFeO_3$ multiferroic materials," *Physica B: Condensed Matter*, vol. 571, pp. 199–203, 2019.

[20] G. Shabbir, A. H. Qureshi, and K. Saeed, "Nano-crystalline LaFeO3 powders synthesized by the citrate-gel method," *Materials Letters*, vol. 60, no. 29–30, pp. 3706–3709, 2006.

[21] D. Çoban Özkan, A. Türk, and E. Çelik, "Synthesis and characterizations of sol–gel derived LaFeO3 perovskite powders," *Journal of Materials Science: Materials in Electronics*, vol. 31, no. 24, pp. 22789–22809, 2020.

[22] M. Muneeswaran, P. Jegatheesan, and N. V. Giridharan, "Synthesis of nanosized BiFeO3 powders by co-precipitation method," *Journal of Experimental Nanoscience*, vol. 8, no. 3, pp. 341–346, 2013.

[23] X. Wang, C. Yang, D. Zhou, Z. Wang, and M. Jin, "Chemical co-precipitation synthesis and properties of pure-phase BiFeO3," *Chemical Physics Letters*, vol. 713, no. September, pp. 185–188, 2018.

[24] M. Khorasani-Motlagh, M. Noroozifar, M. Yousefi, and S. Jahani, "Chemical synthesis and characterization of perovskite NdfeO3 nanocrystals via a Co-precipitation method," *International Journal of NanoScience and Nanotechnology*, vol. 9, no. 1, pp. 7–14, 2013.

[25] W. Haron, A. Wisitsoraat, U. Sirimahachai, and S. Wongnawa, "A simple synthesis and characterization of LaMo3 (M=Al, Co, Fe, Gd) perovskites via chemical coprecipitation method," *Songklanakarin Journal of Science and Technology*, vol. 40, no. 3, pp. 484–491, 2018.

[26] J. A. Gómez-Cuaspud, E. Vera-López, J. B. Carda-Castelló, and E. Barrachina-Albert, "Onestep hydrothermal synthesis of LaFeO3 perovskite for methane steam reformin," *Eaction Kinetics, Mechanisms and Catalysis*, vol. 120, no. 1, pp. 167–179, 2017.

[27] X. Yang, G. Xu, Z. Ren et al., "The hydrothermal synthesis and formation mechanism of single-crystalline perovskite $BiFeO_3$ microplates with dominant (012) facets," *CrystEngComm*, vol. 16, no. 20, pp. 4176–4182, 2014.

[28] M. S. Sazali, M. K. Yaakob, Z. Mohamed et al., "Chitosan-assisted hydrothermal synthesis of multiferroic $BiFeO_3$: effects on structural, magnetic and optical properties," *Results in Physics*, vol. 15, Article ID 102740, 2019.

[29] A. Syed, A. Siddaramanna, A. M. Elgorban, D. A. Hakeem, and G. Nagaraju, "Hydrogen peroxide-assisted hydrothermal synthesis of $bifeo_3$ microspheres and their dielectric behavior," *Magnetochemistry*, vol. 6, no. 3, pp. 42–48, 2020.

[30] Z. Chen, Y. Wu, and J. Hu, "Ethanol-assisted hydrothermal synthesis and characterization of BiFeO $_3$ nanopowders," *Journal of the American Ceramic Society*, vol. 96, no. 5, pp. 1345–1348, 2013.

[31] L. J. Di, H. Yang, T. Xian et al., "Growth of $BiFeO_3$Microcylinders under a hydrothermal condition," *Journal of Nanomaterials*, vol. 2015, no. 3, 5 pages, 2015.

[32] G. Biasotto, A. Z. Simões, C. R. Foschini, M. A. Zaghete, J. A. Varela, and E. Longo, "Microwave-hydrothermal synthesis of perovskite bismuth ferrite nanoparticles," *Materials Research Bulletin*, vol. 46, no. 12, pp. 2543–2547, 2011.

[33] M. Mesbah, S. Hamedshahraki, S. Ahmadi, M. Sharifi, and C. A. Igwegbe, "Hydrothermal synthesis of $LaFeO_3$ nanoparticles adsorbent: characterization and application of error functions for adsorption of fluoride," *MethodsX*, vol. 7, Article ID 100786, 2020.

[34] I. Fernández-Barahona, M. Muñoz-Hernando, and F. Herranz, "Microwave-driven synthesis of iron-oxide nanoparticles for molecular imaging," *Molecules*, vol. 24, no. 7, p. 1224, 2019.

[35] S. Komarneni, "Microwave synthesis of BiFeO3 and CsAl2PO6," *American Ceramic Society*, vol. 79, no. 5, pp. 1409–1412, 1996.

[36] U. A. Joshi, J. S. Jang, P. H. Borse, and J. S. Lee, "Microwave synthesis of single-crystalline perovskite $BiFeO_3$ nanocubes for photoelectrode and photocatalytic applications," *Applied Physics Letters*, vol. 92, no. 24, p. 242106, 2008.

[37] X. Zhu, Q. Hang, Z. Xing et al., "Microwave hydrothermal synthesis, structural characterization, and visiblelight photocatalytic activities of single-crystalline bismuth ferric nanocrystals," *Journal of the American Ceramic Society*, vol. 94, no. 8, pp. 2688–2693, 2011.

[38] F. S. Galasso, *Structure, Properties and Preparation of Perovskite-type Compounds*, R. Smoluchowski and N. Kurti, Eds., 2, pp. 3–49, Pergamon Press, New York, 1st ed edition, 1969.

[39] M. Marezio and P. D. Dernier, "The bond lengths in LaFeO3," *Materials Research Bulletin*, vol. 6, no. 1, pp. 23–29, 1971.

[40] E. A. Kotomin, A. Kuzmin, J. Purans et al., "Theoretical and experimental studies of charge ordering in $CaFeO_3$ and $SrFeO_3$ crystals," *Physica Status Solidi (B)*, vol. 259, no. 1, Article ID 2100238, 2022.

[41] N. Wang, X. Luo, L. Han et al., "Structure, performance, and application of $BiFeO_3$ nanomaterials," *Nano-Micro Letters*, vol. 12, no. 1, p. 81, 2020.

[42] R. Maity, A. Dutta, S. Halder, S. Shannigrahi, K. Mandal, and T. P. Sinha, "Enhanced photocatalytic activity, transport properties and electronic structure of Mn doped GdFeO3 synthesized using the sol–gel process," *Physical Chemistry Chemical Physics*, vol. 23, no. 30, pp. 16060–16076, 2021.

[43] C. S. Bongu, J. Ragupathi, and K. Nallathamby, "Exploration of MnFeO3/multiwalled carbon nanotubes composite as potential anode for lithium ion batteries," *Inorganic Chemistry*, vol. 55, no. 22, pp. 11644–11651, 2016.

[44] S. Phokha, S. Pinitsoontorn, S. Maensiri, and S. Rujirawat, "Structure, optical and magnetic properties of LaFeO3 nanoparticles prepared by polymerized complex method,"

Journal of Sol-Gel Science and Technology, vol. 71, no. 2, pp. 333–341, 2014.

[45] S. Sumithra and N. V. Jaya, "Structural, optical and magnetization studies of Fe-doped CaSnO3 nanoparticles via hydrothermal route," *Journal of Materials Science: Materials in Electronics*, vol. 29, no. 5, pp. 4048–4057, 2018.

[46] J. Wang, J. B. Neaton, H. Zheng et al., "Epitaxial BiFeO3 multiferroic thin film heterostructures," *Science 84*, vol. 299, no. 5613, pp. 1719–1722, 2003.

[47] T. Park, G. C. Papaefthymiou, A. J. Viescas, A. R. Moodenbaugh, and S. S. Wong, *SizeDependent Magnetic Properties of Nanoparticles*, ACS, Washington, USA, 2007.

[48] J. Jiang, J. Zou, M. N. Anjum et al., "Synthesis and characterization of wafer-like BiFeO3 with efficient catalytic activity," *Solid State Sciences*, vol. 13, no. 9, pp. 1779–1785, 2011.

[49] X. Luo, W. Xing, Z. Li, G. Wu, and X. Chen, "Impact of the Fe doping on magnetism in perovskite cobaltites," *Physical Review B: Condensed Matter*, vol. 75, no. 5, Article ID 054413, 2017.

[50] V. Rao Bakshi, B. V. Prasad, N. R. Gade, F. C. Chou, and S. Babu Devarasetty, "Magnetic properties of Fe doped SmCrO3 perovskite," *AIP Conference Proceedings*, vol. 54, p. 1735, 2014.

[51] M. R. Manju, V. P. Kumar, and V. Dayal, "Investigation of ferromagnetic properties in Fe/Co substituted $BaSnO_3$ perovskite stannates," *Physica B: Condensed Matter*, vol. 500, pp. 14–19, 2016.

[52] P. I. Cowin, C. T. G. Petit, R. Lan, J. T. S. Irvine, and S. W. Tao, "Recent progress in the development of anode materials for solid oxide fuel cells," *Advanced Energy Materials*, vol. 1, no. 3, pp. 314–332, 2011.

[53] M. Nisar, Y. Ma, S. Khan et al., "Predicted half-metallicity and ferromagnetismin the Fe (III) doped BaZrO3perovskite: A theoretical insight," *AIP Advances*, vol. 2021, Article ID 055104, 2021.

[54] A. Rajamani, G. F. Dionne, D. Bono, and C. Ross, "Faraday rotation, ferromagnetism, and optical properties in Fe-doped BaTiO3," *Journal of Applied Physics*, vol. 98, no. 6, p. 063907, 2005.

[55] P. V. Anikina, A. A. Markov, M. V. Patrakeev, I. A. Leonidov, and V. L. Kozhevnikov, "High-temperature transport and stability of SrFe1−xNbxO3−δ," *Solid State Sciences*, vol. 11, no. 6, pp. 1156–1162, 2009.

[56] R. Lan, P. I. Cowin, S. Sengodan, and S. Tao, "A perovskite oxide with high conductivities in both air and reducing atmosphere for use as electrode for solid oxide fuel cells," *Scientific Reports*, vol. 6, no. 1, Article ID 31839, 2016.

[57] N. T. Hung, L. H. Bac, N. N. Trung, N. T. Hoang, P. Van Vinh, and D. D. Dung, "Room-temperature ferromagnetism in Fe-based perovskite solid solution in lead-free ferroelectric $Bi_{0.5}Na_{0.5}TiO_3$ materials," *Journal of Magnetism and Magnetic Materials*, vol. 451, pp. 183–186, 2018.

[58] V. Guigoz, L. Balan, A. Aboulaich, R. Schneider, and T. Gries, "Heterostructured thin LaFeO3/g-C3N4 films for efficient photoelectrochemical hydrogen evolution," *International Journal of Hydrogen Energy*, vol. 45, no. 35, pp. 17468–17479, 2020.

[59] G. Iervolino, V. Vaiano, D. Sannino, L. Rizzo, and P. Ciambelli, "Production of hydrogen from glucose by LaFeO3 based photocatalytic process during water treatment," *International Journal of Hydrogen Energy*, vol. 41, no. 2, pp. 959–966, 2016.

[60] I. M. Nassar, S. Wu, L Liang, and X. Li, "Facile preparationof, 2018 of n -type LaFeO3 perovskite film for efficient photoelectrochemical water splitting," *Chemistry Select*, vol. 3, pp. 968–972, 2018.

[61] M. Ismael and M. Wark, "Perovskite-type LaFeO3: photoelectrochemical properties and photocatalytic degradation of organic pollutants under visible light irradiation," *Catalysts*, vol. 9, no. 4, p. 342, 2019.

[62] B. M. Pirzada, R. K. Kunchala, R. K. Kunchala, and B. S. Naidu, "Synthesis of $LaFeO_3/Ag_2CO_3$ nanocomposites for photocatalytic degradation of rhodamine B and p-chlorophenol under natural sunlight," *ACS Omega*, vol. 4, no. 2, pp. 2618–2629, 2019.

[63] T. Vijayaraghavan, R. Althaf, P. Babu, K. M. Parida, S. Vadivel, and A. M. Ashok, "Visible light active LaFeO3 nano perovskite-RGO-NiO composite for efficient H2 evolution by photocatalytic water splitting and textile dye degradation," *Journal of Environmental Chemical Engineering*, vol. 9, no. 1, Article ID 104675, 2021.

[64] D. Singh, T. Tabari, M. Ebadi, M. Trochowski, M. Baris Yagci, and W. Macyk, "Efficient synthesis of $BiFeO_3$ by the microwave-assisted sol-gel method: "A" site influence on the photoelectrochemical activity of perovskites," *Applied Surface Science*, vol. 471, pp. 1017–1027, 2019.

[65] B.-J. Kim, E. Fabbri, D. F. Abbott et al., "Functional role of Fe-doping in Co-based perovskite oxide catalysts for oxygen evolution reaction," *Journal of the American Chemical Society*, vol. 141, no. 13, pp. 5231–5240, 2019.

[66] J. Gao, Y. Zhang, X. Wang et al., "Nitrogen-doped Sr2Fe1.5Mo0.5O6-δ perovskite as an efficient and stable catalyst for hydrogen evolution reaction," *Materials Today Energy*, vol. 20, Article ID 100695, 2021.

[67] H. Chang, E. Bjorgum, O. Mihai et al., "Effects of oxygen mobility in La-Fe-based perovskites on the catalytic activity and selectivity of methane oxidation," *ACS Catalysis*, vol. 10, no. 6, pp. 3707–3719, 2020.

[68] V. Lantto, S. Saukko, N. N. Toan, L. F. Reyes, and C. G. Granqvist, "Gas sensing with perovskite-like oxides having ABO_3 and BO $_3$ structures," *Journal of Electroceramics*, vol. 13, no. 1-3, pp. 721–726, 2004.

[69] F. Zaza, V. Pallozzi, and E. Serra, "Optimization of working conditions for perovskite-based gas sensor devices by multiregression analysis," *Journal of Nanotechnology*, vol. 2019, pp. 1–19, 2019.

[70] A. Jamil, S. Fareed, F. Afsar, F. Siddique, F. Sher, and M. A. Rafiq, "Development of high performance Bi5Ti3-FeO15 layered perovskite oxygen gas sensor and its dielectric behavior," *Materials Research Express*, vol. 6, pp. 115028–11, 2019.

[71] X. Wang, H. Qin, J. Pei et al., "Sensing performances to low concentration acetone for palladium doped LaFeO3 sensors," *Journal of Rare Earths*, vol. 34, no. 7, pp. 704–710, 2016.

[72] X. Wang, H. Qin, L. Sun, and J. Hu, "CO2 sensing properties and mechanism of nanocrystalline LaFeO3 sensor," *Sensors and Actuators B: Chemical*, vol. 188, pp. 965–971, 2013.

[73] E. Cao, H. Wang, X. Wang et al., "Enhanced ethanol sensing performance for chlorine doped nanocrystalline LaFeO3-powders by citric sol-gel method," *Sensors and Actuators B: Chemical*, vol. 251, pp. 885–893, 2017.

[74] L. Ma, S. Ma, X. Shen et al., "PrFeO3 hollow nanofibers as a highly efficient gas sensor for acetone detection," *Sensors and Actuators B: Chemical*, vol. 255, pp. 2546–2554, 2018.

[75] M. Chen, Y. Zhang, J. Zhang et al., "Facile lotus-leaf-templated synthesis and enhanced xylene gas sensing properties

of Ag-LaFeO3 nanoparticles," *J. Mater. Chem. C*, vol. 6, no. 23, pp. 6138–6145, 2018.

[76] T. Han, S. Ma, X. Xu et al., "Rough SmFeO3 nanofibers as an optimization ethylene glycol gas sensor prepared by electrospinning," *Materials Letters*, vol. 268, p. 127575, 2020.

[77] W. Wei, S. Guo, C. Chen et al., "High sensitive and fast formaldehyde gas sensor based on Ag-doped LaFeO3nanofibers," *Journal of Alloys and Compounds*, vol. 695, pp. 1122–1127, 2017.

[78] K. Yang, J. Ma, X. Qiao, Y. Cui, L. Jia, and H. Wang, "Hierarchical porous LaFeO3 nanostructure for efficient trace detection of formaldehyde," *Sensors and Actuators B: Chemical*, vol. 313, p. 128022, 2020.

[79] A. Queraltó, D. Graf, R. Frohnhoven et al., "LaFeO3 nanofibers for high detection of sulfur-containing gases," *ACS Sustainable Chemistry & Engineering*, vol. 7, no. 6, pp. 6023–6032, 2019.

[80] H. E. Kan, Y. F. Zhao, Y. J. Liu, Y. H. Li, and H. Y. Zhao, "Synthesis, characterisation and sensing properties of perovskite EuFe 0.9Co 0.1O 3 materials," *Materials Technology*, vol. 27, no. 1, pp. 136–138, 2012.

[81] S. B. Arindam Bala, M. D. Majumder, and R. C. Ayan, "Hydrogen sensing characteristics of perovskite based calcium doped BiFeO3 thin films," *Journal of Hydrogen Energy*, vol. 44, no. 33, pp. 18648–18656.

[82] S. Chakraborty and M. Pal, "Highly efficient novel carbon monoxide gas sensor based on bismuth ferrite nanoparticles for environmental monitoring," *New Journal of Chemistry*, vol. 42, no. 9, pp. 7188–7196, 2018.

[83] S. Das, S. Rana, S. M. Mursalin, P. Rana, and A. Sen, "Sonochemically prepared nanosized BiFeO3 as novel SO2 sensor," *Sensors and Actuators B: Chemical*, vol. 218, pp. 122–127, 2015.

[84] T. Tasaki, S. Takase, and Y. Shimizu, "Fabrication of Sm-based perovskite-type oxide ThinFilms and gas sensing properties to acetylene," *Journal of Sensor Technology*, vol. 02, no. 02, pp. 75–81, 2012.

[85] S. Thirumalairajan, K. Girija, V. R. Mastelaro, and N. Ponpandian, "Surface morphologydependent room-temperature LaFeO3 nanostructure thin films as selective NO2 gas sensor prepared by radio frequency magnetron sputtering," *ACS Applied Materials & Interfaces*, vol. 6, no. 16, pp. 13917–13927, 2014.

[86] M. Renu, M. Agarwal, and K. Singh, "Heavy metal removal from wastewater using various adsorbents: a review," *Journal of Water Reuse and Desalination*, vol. 7, no. 4, pp. 387–419, 2017.

[87] V. Andal and G. Buvaneswari, "Removal of lead ions by NiFe2O4 nanoparticles," *IJRET*, vol. 03, no. 01, pp. 475–483, 2014.

[88] G. Jayanthi, S. Sumathi, and V. Andal, "Synthesis and applications of perovskite in heavy metal ions removal-a brief perspective," *Materials Today Proceedings*, vol. 55, pp. 201–211, 2022.

[89] Z. N. Garba, W. Zhou, M. Zhang, and Z. Yuan, "A review on the preparation, characterization and potential application of perovskites as adsorbents for wastewater treatment," *Chemosphere*, vol. 244, Article ID 125474, 2020.

[90] A. B. La and I. Processes, "The sorption performance of cetyl trimethyl," *Molecules*, vol. 25, pp. 1–15, 2020.

[91] M. Y. Leiw, G. H. Guai, X. Wang, M. S. Tse, C. M. Ng, and O. K. Tan, "Dark ambient degradation of Bisphenol A and Acid Orange 8 as organic pollutants by perovskite SrFeO3-δdoi: 10.1016/j.seppur.2019.116195. metal oxide," *Journal of Hazardous Materials*, vol. 260, pp. 1–8, 2013.

[92] M. D. Luu, N. N. Dao, D. Van Nguyen, N. C. Pham, T. N. Vu, and T. D. Doan, "A new perovskite-type NdFeO 3 adsorbent: synthesis , characterization , and as (V) adsorption," *Advances in Natural Sciences: Nanoscience and Nanotechnology*, vol. 7, no. 2, p. 025015, 2016.

[93] Y. Wei, H. Liu, C. Liu et al., "Fast and efficient removal of As(III) from water by CuFe2O4 with peroxymonosulfate: effects of oxidation and adsorption," *Water Research*, vol. 150, no. Iii, pp. 182–190, 2019.

[94] H. Deng, Z. Mao, H. Xu, L. Zhang, Y. Zhong, and X. Sui, "Synthesis of fibrous LaFeO3 perovskite oxide for adsorption of Rhodamine B," *Ecotoxicology and Environmental Safety*, vol. 168, no. March 2018, pp. 35–44, 2019.

[95] H. Tavakkoli and F. Hamedi, "Synthesis of Gd0.5Sr0.5FeO3 perovskite-type nanopowders for adsorptive removal of MB dye from water," *Research on Chemical Intermediates*, vol. 42, no. 4, pp. 3005–3027, 2015.

[96] S. Thirumalairajan, K. Girija, V. R. Mastelaro, and N. Ponpandian, "Photocatalytic degradation of organic dyes under visible light irradiation by floral-like LaFeO3 nanostructures comprised of nanosheet petals," *New Journal of Chemistry*, vol. 38, no. 11, pp. 5480–5490, 2014.

[97] H. Neville and D. Bavelier, "Human brain plasticity: evidence from sensory deprivation and altered language experience," *Progress in Brain Research*, vol. 138, pp. 177–188, 2002.

[98] R. Guo, L. Fang, W. Dong, F. Zheng, and M. Shen, "Enhanced photocatalytic activity and ferromagnetism in Gd doped BiFeO 3 nanoparticles," *Journal of Physical Chemistry C*, vol. 114, no. 49, pp. 21390–21396, 2010.

[99] Y. N. Feng, H. C. Wang, Y. D. Luo, Y. Shen, and Y. H. Lin, "Ferromagnetic and photocatalytic behaviors observed in Ca-doped $BiFeO_3$ nanofibres," *Journal of Applied Physics*, vol. 113, no. 14, p. 146101, 2013.

[100] Z. H. Jaffari, S. M. Lam, J. C. Sin, H. Zeng, and A. R. Mohamed, "Magnetically recoverable Pd-loaded BiFeO3 microcomposite with enhanced visible light photocatalytic performance for pollutant, bacterial and fungal elimination," *Separation and Purification Technology*, vol. 236, Article ID 116195, 2020.

[101] V. Sydorchuk, I. Lutsyuk, V. Shved et al., "PrCo1−xFexO3 perovskite powders for possible photocatalytic applications," *Research on Chemical Intermediates*, vol. 46, no. 3, pp. 1909–1930, 2020.

[102] P. Dhanasekaran and N. M. Gupta, "Factors affecting the production of H 2 by water splitting over a novel visible-light-driven photocatalyst GaFeO 3," *International Journal of Hydrogen Energy*, vol. 37, no. 6, pp. 4897–4907, 2012.

[103] X. Lü, J. Xie, H. Shu, J. Liu, C. Yin, and J. Lin, "Microwaveassisted synthesis of nanocrystalline YFeO3 and study of its photoactivity," *Materials Science and Engineering: B*, vol. 138, no. 3, pp. 289–292, 2007.

[104] Y. Yang, Q. Chen, Z. Yin, and J. Li, "Study on the photocatalytic activity of K2La2Ti3O10 doped with vanadium (V)," *Journal of Alloys and Compounds*, vol. 488, no. 1, pp. 364–369, 2009.

[105] O. V. Nkwachukwu and O. A. Arotiba, "Perovskite oxide–based materials for photocatalytic and photoelectrocatalytic treatment of water," *Frontiers of Chemistry*, vol. 9, Article ID 634630, 2021.

[106] J. Xia, S. Yin, H. Li, H. Xu, L. Xu, and Y. Xu, "Improved visible light photocatalytic activity of sphere-like BiOBr hollow and porous structures synthesized via a reactable

ionic liquid," *Dalton Transactions*, vol. 40, no. 19, pp. 5249–5258, 2011.

[107] S. Thirumalairajan, K. Girija, N. Y. Hebalkar, D. Mangalaraj, C. Viswanathan, and N. Ponpandian, "Shape evolution of perovskite LaFeO3 nanostructures: a systematic investigation of growth mechanism, properties and morphology dependent photocatalytic activities," *RSC Advances*, vol. 3, no. 20, p. 7549, 2013.

[108] Z. Hu, D. Chen, S. Wang, N. Zhang, L. Qin, and Y. Huang, "Facile synthesis of Sm-doped BiFeO3 nanoparticles for enhanced visible light photocatalytic performance," *Materials Science and Engineering: B*, vol. 220, pp. 1–12, 2017.

[109] A. Haruna, I. Abdulkadir, and S. O. Idris Synthesis, "Characterization and photocatalytic properties of Bi0.85-XMXBa0.15FeO3 (M = Na and K, X=0, 0.1) perovskite-like nanoparticles using the sol- gel method," *Journal of King Saud University Science*, vol. 20197 pages, 2019.

[110] Z. H. Jaffari, S. M. Lam, J. C. Sin, and H. Zeng, "Boosting visible light photocatalytic and antibacterial performance by decoration of silver on magnetic spindle-like bismuth ferrite," *Materials Science in Semiconductor Processing*, vol. 101, pp. 103–115, 2019.

[111] M. Sakar, S. Balakumar, P. Saravanan, and S. Bharathkumar, "Compliments of confinements: substitution and dimension induced magnetic origin and band bending mediated photocatalytic enhancements in Bi 1-xDyxFeO3 particulate and fiber nanostructures," *Nanoscale*, vol. 7, no. 24, pp. 10667–10679, 2015.

[112] K. F. Moura, L. Chantelle, D. . Rosendo, E. Longo, and I. M. G. d Santos, "Effect of Fe3+ doping in the photocatalytic properties of BaSnO3 perovskite," *Materials Research*, vol. 20, no. suppl 2, pp. 317–324, 2017.

[113] O. V. Nkwachukwu, C. Muzenda, B. O. Ojo et al., "Photoelectrochemical degradation of organic pollutants on a La3+ doped BiFeO3 perovskite," *Catalysts*, vol. 11, no. 9, p. 1069, 2021.

[114] Y. W. Chen, J. L. Kuo, and K. H. Chew, "Polar ordering and structural distortion in electronic domain-wall properties of BiFeO3," *Journal of Applied Physics*, vol. 122, no. 7, Article ID 075103, 2017.

[115] S. Upadhyay, J. Shrivastava, A. Solanki et al., "Enhanced photoelectrochemical response of BaTiO3 with Fe doping: experiments and first-principles analysis," *Journal of Physical Chemistry C*, vol. 115, no. 49, pp. 24373–24380, 2011.

[116] D. Cao, Z. Wang, V. Nasori, L. Wen, Y. Mi, and Y. Lei, "Switchable charge- transfer in the photoelectrochemical energy-conversion process of ferroelectric BiFeO3 photoelectrodes," *Angewandte Chemie*, vol. 126, no. 41, pp. 11207–11211, 2014.

[117] P. Mehdizadeh, O. Amiri, S. Rashki, M. Salavati-Niasari, M. Salimian, and L. K. Foong, "Effective removal of organic pollution by using sonochemical prepared LaFeO3 perovskite under visible light," *Ultrasonics Sonochemistry*, vol. 61, Article ID 104848, 2020.

[118] O. Mihai, D. Chen, and A. Holmen, "Chemical looping methane partial oxidation: the effect of the crystal size and O content of LaFeO 3," *Journal of Catalysis*, vol. 293, pp. 175–185, 2012.

[119] M. Mokhtar, A. Medkhali, K. Narasimharao, and S. Basahel, "Divalent transition metals substituted LaFeO3 perovskite catalyst for nitrous oxide decomposition," *Journal of Membrane and Separation Technology*, vol. 3, no. 4, pp. 206–212, 2014.